A&A 522, A90 (2010)
DOI: 10.1051/0004-6361/201014774

Astronomy & Astrophysics

Experimental studies of the dissociative recombination of CD_3CDOD^+ and $CH_3CH_2OH_2^+$

M. Hamberg[1], V. Zhaunerchyk[1,2], E. Vigren[1], M. Kaminska[3], I. Kashperka[1], M. Zhang[4], S. Trippel[5], F. Österdahl[1], M. af Ugglas[1], R. D. Thomas[1], A. Källberg[6], A. Simonsson[6], A. Paál[6], J. Semaniak[3], M. Larsson[1], and W. D. Geppert[1]

[1] Department of Physics, Stockholm University, 106 91 Stockholm, Sweden
e-mail: mh@physto.se
[2] Radboud University Nijmegen, Institute for Molecules and Materials, PO Box 9010, 6500 GL Nijmegen, The Netherlands
[3] Institute of Physics, Jan Kochanowski University, Świętokrzyska 15, 25406 Kielce, Poland
[4] Institute of Modern Physics, Chinese Academy of Sciences, 509 Nanchang Rd., Lanzhou 730000, PR China
[5] Department of Physics, Albert-Ludwigs Universität Freiburg, Hermann-Herder-Str. 3, 79104 Freiburg Germany
[6] Manne Siegbahn Laboratory, Frescativägen 26, 114 18 Stockholm, Sweden

Received 12 April 2010 / Accepted 22 July 2010

ABSTRACT

Aims. We determine branching fractions, cross sections and thermal rate constants for the dissociative recombination of CD_3CDOD^+ and $CH_3CH_2OH_2^+$ at the low relative kinetic energies encountered in the interstellar medium.
Methods. The experiments were carried out by merging an ion and electron beam at the heavy ion storage ring CRYRING, Stockholm, Sweden.
Results. Break-up of the CCO structure into three heavy fragments is not found for either of the ions. Instead the CCO structure is retained in $23 \pm 3\%$ of the DR reactions of CD_3CDOD^+ and $7 \pm 3\%$ in the DR of $CH_3CH_2OH_2^+$, whereas rupture into two heavy fragments occurs in $77 \pm 3\%$ and $93 \pm 3\%$ of the DR events of the respective ions. The measured cross sections were fitted between 1–200 meV yielding the following thermal rate constants and cross-section dependencies on the relative kinetic energy: $\sigma(E_{\rm cm}[\rm eV]) = 1.7 \pm 0.3 \times 10^{-15}(E_{\rm cm}[\rm eV])^{-1.23\pm0.02}$ cm^2 and $k(T) = 1.9 \pm 0.4 \times 10^{-6}(T/300)^{-0.73\pm0.02}$ cm^3 s^{-1} for $CH_3CH_2OH_2^+$ as well as $k(T) = 1.1 \pm 0.4 \times 10^{-6}(T/300)^{-0.74\pm0.05}$ cm^3 s^{-1} and $\sigma(E_{\rm cm}[\rm eV]) = 9.2 \pm 4 \times 10^{-16}(E_{\rm cm}[\rm eV])^{-1.24\pm0.05}$ cm^2 for CD_3CDOD^+

Key words. astrochemistry – molecular processes – plasmas – methods: laboratory

1. Introduction

Ion reactions play an important role as steps in the synthesis of many important molecules found in the interstellar medium. Presently 151 molecular species have been detected in space (astrochemistry.net 2009). This amount is steadily increasing creating the need to devise formation routes for these molecules and to distinguish between feasible and unfeasible synthesis pathways under the different physical and chemical conditions found in different astronomical objects. Reactions involving ions including (but not limited to) association, ionization and recombination contribute to the intricate reaction networks that form the backbone of state-of-the-art astrochemical model calculations. Changes in the rates of one single process might drastically alter the predicted abundances of one or more species. Many processes have been well characterised by experimental studies, whereas others could successfully be investigated by ab-initio calculations. However, recombination reactions of larger ions with electrons, such as dissociative recombination (DR) do not fall under these categories.

DR is the process where a free electron recombines with a molecular ion to form an excited neutral that disintegrates into two or more neutral fragments in order to release the excess energy gained through the electron attachment. It is one of the dominating ionisation reducing reactions in many natural environments, such as interstellar cloud cores (Boger & Sternberg 2006; Florescu-Mitchell & Mitchell 2006; Thomas 2008) and the comae of comets (Haider & Bhardwaj 2005), and also plays an important role in aurorae (Peterson et al. 1994), aeronomical plasmas (Yee et al. 1989), and lightning (Smirnova et al. 2002). DR is also a crucial process in man-made plasmas such as those present in combustion engines and fusion reactors (Florescu-Mitchell & Mitchell 2006). It is very efficient under cold conditions and therefore ubiquitous in interstellar environments such as dark clouds. Although DR reactions are omnipresent in plasmas and thus crucial processses in these environments, product branching ratios of DR reactions have proven to be very unpredictable and present one of the great remaining challenges for theoreticians (see e.g. Geppert & Larsson 2008). To elucidate these completely by experimental methods is also far from trivial and it was as late as in the 1990s when Datz et al. (1995) ingeniously applied the technique of merged ion electron beams using a storage ring in conjunction with a previously invented grid technique (Mitchell et al. 1982) to obtain solid information about these distributions. Subsequently, heavy-ion storage rings like ASTRID (Denmark), TSR (Heidelberg) and CRYRING (Stockholm, Sweden) have been successfully used as tools for investigations of astrophysically relevant DR reactions (see e.g. Larsson et al. 1993, 1995; Al-Khalili et al. 1998; Neau et al. 2000; McCall et al. 2003; Hamberg et al. 2005; Geppert et al. 2005; Geppert & Larsson 2008; Thomas 2008; Andersen et al. 1996; Jensen et al. 2000; Kreckel et al. 2005; Nevo et al. 2007). However, such time-consuming experiments are restricted to a few places over the world and investigators are

therefore often struggling to meet the dire need of experimental data from astrochemical modelers.

Ethanol has been found in hot cores (Schilke et al. 1997; MacDonald et al. 1996) and Tielens & Charnley (1997) proposed that this substance could be formed in these objects by C addition to CO and successive hydrogenation on mantles of interstellar grains in these objects. Bisschop et al. (2007) later experimentally showed that production of ethanol occurs through H-bombardment of CH_3CHO-containing ices, in which up to 20% of the acetaldehyde was hydrogenated to ethanol. However, if CH_2CO, CH_3CHO and C_2H_5OH would be interconnected through processes on the surfaces of dust grains, the same spatial abundance distributions would be expected for all three species. Such a pattern was not observed in astronomical observations of IRAS 16292–2422 which implied that the suggested hydrogenation reactions on grain surfaces alone cannot account for the observed abundances of ethanol (Bisschop et al. 2008). An alternative gas phase pathway could be the formation through association of e.g. $H_3O^+ + C_2H_4$ followed by DR of the generated $C_2H_5OH_2^+$ ion. However, previous DR investigations of the lighter homologue of the title substance, namely protonated methanol, showed that only a very small fraction (3%) of DR processes lead to the unprotonated species. It is therefore reasonable to assume a similar behaviour in the case of protonated ethanol ($C_2H_5OH_2^+$) although due to the unpredictable behaviour of DR processes experimental determination of branching fractions are necessary to support such claims.

Investigations into the DR of the fully deuterated and deuteronated acetaldehyde cation (CD_3CDOD^+) and protonated ethanol ($CH_3CH_2OH_2^+$) cations have been undertaken at the heavy ion storage ring CRYRING. In this Paper we present experimental results on the cross-section, rate constant and branching fractions between channels breaking and retaining the CCO structure.

2. Experiment

The experiments were performed at the heavy ion storage ring CRYRING at the Manne Siegbahn Laboratory in Stockholm, Sweden. The ring consists of twelve straight segments separated by bending magnets and has a circumference of ~51.6 m. The experiment has previously been described in detail (see e.g. Neau et al. 2000) and is therefore only briefly summarized here.

The $CH_3CH_2OH_2^+$ ion was produced from a gas mixture of ethanol and pure hydrogen gas, whereas the CD_3CDOD^+ ion was generated through fragmentation of fully deuterated ethanol. The deuterated isotopologue was used in the hope of obtaining a better mass resolution between the fragments and thus being able to elucidate the full branching fractions. The ionization was performed by a high voltage discharge in a hollow-cathode ion source. The ions were then accelerated to 40 keV energy from the source and mass-selected by a bending magnet. After injection into the storage ring they were further accelerated by a driven (non-resonant) drift-tube system until they reached the maximum energy $\sim 96/m_{\rm ion}$ MeV (where $m_{\rm ion}$ is the ion mass in amu) after about one second. Long storage lifetimes of several seconds and minimization of rest gas collisions are ensured by the ultra high vacuum in the ring ($\sim 10^{-11}$ Torr).

An electron cooler that generates a beam of cold electrons with a diameter of 40 mm and a 2 meV transversal energy spread is located in one of the straight sections. The electron beam is bent in to overlap the ions for ~85 cm, bent out at the end of this region and collected by an anode. Neutral products generated by DR reactions in this interaction region will then leave the ring tangentially unaffected by the bending magnet and enter a side arm of the ring where they are detected by means of an ion-implanted silicon detector (IID). The electron cooler also helps to slightly reduce the velocity spread of the ions through Coulomb drag-force effects between the ions and the electrons. This generally leads to shrinking of the phase-space occupied by the ions, however, due to their large mass this effect is negligible for the ions studied here. Vibrationally excited states of the ions that are possibly created in the ion source are radiatively cooled down through IR-active modes (typically on a timescale of 0.1–1 s) whereas ions vibrationally excited into IR-inactive modes can be cooled by super elastic scattering of electrons in the cooler (Wolf et al. 2003).

2.1. Branching fractions measurement

The branching fractions for the different DR reaction channels were measured at a nominal collision energy of ~0 eV. This implies that ions and electrons are traveling with the same mean velocity. The IID detecting the neutrals created in the interaction region is energy-sensitive. Due to the uniform, very well-defined velocity of the ions, the detected signal will be directly proportional to the mass of the fragments. The velocity difference of the fragments produced by the DR process is negligible compared with the traveling speed of the ions. Therefore, the different fragments arising from a particular DR event will hit the detector within a time interval that is much shorter than the response time of the detection system. Thus, only signals corresponding to the full ion mass, i.e. the sum of the fragments, are observed and no information about the products is obtained. To solve this issue, a transparent grid with a well-determined transmission probability $P_T = 0.297 \pm 0.015$ is inserted directly in front of the detector. In this case the recorded spectrum splits up into several peaks with energies corresponding to the masses of the fragments which hit the detector (i.e. those fragments passing through the grid). Due to resolution limitations in the detector system, it was not with certainty possible to resolve all fragment masses (especially those differing only by one or two amu) and therefore, we are restricted to distinguishing only between reaction channels leading to fragments containing a different numbers of heavier atoms (C and O).

The experiment consisted of four parts:

i) measurement of the fragment energy spectrum without the grid and with the electron cooler tuned to a voltage corresponding to zero relative kinetic energy between electrons and ions ($E_{\rm cm}$ =~0 eV);
ii) a spectrum taken without the grid and with the electron cooler cathode set to a voltage corresponding to $E_{\rm cm}$ = 1 eV. At that energy the DR cross section is very small and the count rate is dominated by background events (mostly charge transfer and other reactions induced by collisions of rest gases in the ring);
iii) a spectrum taken with the grid inserted in front of the detector and the electron cooler cathode set to a voltage corresponding to $E_{\rm cm}$ =~ 0 eV;
iv) a spectrum with the grid inserted in front of the detector and the electron cooler cathode set to a voltage corresponding to $E_{\rm cm}$ = 1 eV. Again the count rate is very low and is dominated by products from rest gas collisions.

The pure DR fragment energy distribution was obtained after normalising (with respect to the ion current in the different measurements) and subtracting the spectra recorded at 1 eV $E_{\rm cm}$ from

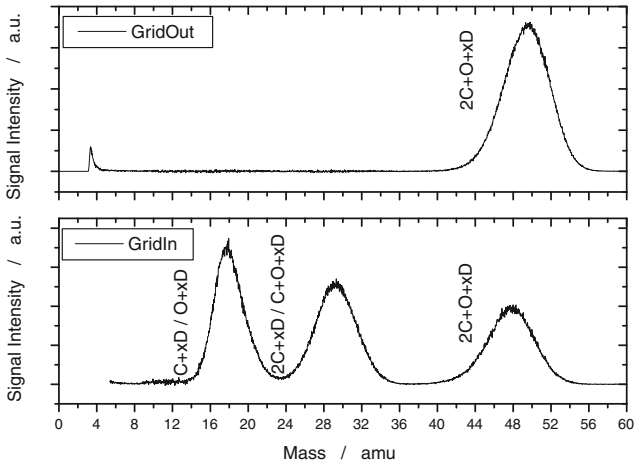

Fig. 1. *Top*: the background subtracted pulse-height spectrum obtained for CD_3CDOD^+ using the IID system without the grid in front of the detector. The large peak at high energy is due to particles impacting at full beam energy. If losses of heavy fragments that miss the detector due to their high transverse energy would occur, one or two smaller peaks at lower energies would indicate that. It is clear that no losses of heavy fragments are observed. The sharp feature at very low mass/energy is due to noise in the detector system. *Bottom*: the background subtracted pulse-height spectrum obtained for CD_3CDOD^+ using the IID system with the grid inserted in front of the detector. The three major peaks are due to signals from passing fragments containing one, two or three heavy atoms, respectively.

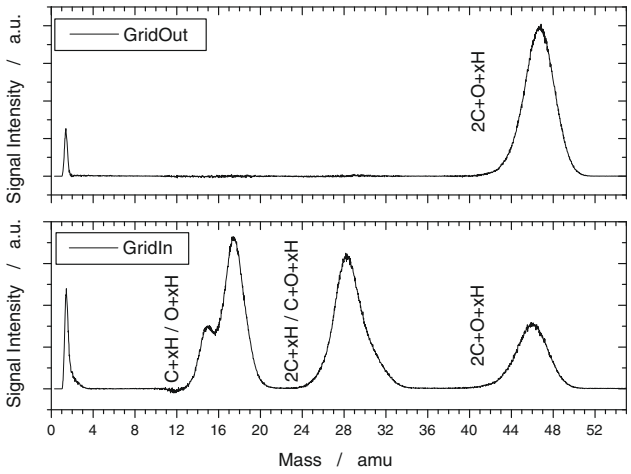

Fig. 2. *Top*: the background subtracted pulse-height spectrum obtained for $CH_3CH_2OH_2^+$ using the IID system without the grid in front of the detector. The large peak at high energy is due to particles impacting at full beam energy. If losses of heavy fragments passing by the detector due to their high transverse energy would occur, one or two smaller peaks at lower energies would indicate that. It is clear that no loss of heavy fragments are observed. The sharp feature at the leftmost position is due to noise in the detector system. *Bottom*: the background subtracted pulse-height spectrum obtained for $CH_3CH_2OH_2^+$ using the IID system with the grid inserted in front of the detector. The three major peaks are due to detection of fragments containing one, two or three heavy atoms, respectively. The sharp feature at very low mass/energy is due to noise in the detector system mixed with signal from hydrogen fragments.

those recorded at 0 eV $E_{\rm cm}$. The X-axis of the spectra was scaled to nominal mass (in amu, calibrated via the position of the full mass and the signal from carbon atoms produced by background events). In the spectra with no grid inserted one should – as previously stated – only observe one peak corresponding to the full ion mass. Signals appearing at lower energies (masses) would indicate that some of the fragments miss the detector due to a high kinetic energy release in the DR reactions. Indeed, in such a spectrum (displayed in top of Figs. 1 and 2) only one major peak is observed and therefore we could conclude that no losses of heavy fragments occurred for any of the ions (the small structures at the low energies/masses are due to detector system noise).

The background-subtracted fragment energy spectra with the grid inserted are shown at the bottom of Figs. 1 and 2. Due to the fragmentation of the ion into the several different neutral products, and the transmission probability of the grid, the spectra now exposes the intensity of all the possible product masses. The peaks correspond to fragments containing one (C or O), two (those with 2C or C+O) or three heavy atoms (2C+O) plus hydrogen/deuterium atoms. To compute the branching fractions from the peak intensities and the transmission probability, P_T, the following matrix system was constructed:

$$\begin{pmatrix} P_T & P_T^2 & P_T^3 \\ 0 & P_T(1-P_T) & 3P_T^2(1-P_T) \\ 0 & P_T(1-P_T) & 3P_T(1-P_T)^2 \end{pmatrix} \begin{pmatrix} N_\alpha \\ N_\beta \\ N_\gamma \end{pmatrix} = \begin{pmatrix} I(2C+O) \\ I(2C, C+O) \\ I(C, O) \end{pmatrix}, \quad (1)$$

where $N_{\alpha-\gamma}$ is the number of counts in each reaction channel, $\alpha-\gamma$ (leading to separation of the CCO-chain into one, two and three heavy fragments, respectively), and I is the total number of counts in each peak. For example, each column in the matrix on the left of Eq. (1) corresponds to a reaction channel. In the middle column, P_T^2 is the probability that both heavy products from reaction channel β pass through the grid and contribute to the full mass energy peak. $P_T(1-P_T)$ in the second and third rows corresponds to the probability that the heavier products (containing C_2 or CO) passes through the grid while the lighter products (containing C or O) are stopped by the grid or vice versa. Since no product channels separating the CCO-chain into three fragments are energetically open for CD_3CDOD^+ the corresponding third column in the matrix was removed in the calculation of the branching fractions for that particular ion. Solving the matrix system shows that break-up of the ion into three fragments which each contain a heavy atom does not occur in the DR of $CH_3CH_2OH_2^+$. Instead, the CCO structure is retained in $23 \pm 3\%$ of the DR events in the case of CD_3CDOD^+ and $7 \pm 3\%$ of those events in the case of $CH_3CH_2OH_2^+$. Rupture into two fragments (containing 2 and 1 heavy atom) was found in $77 \pm 3\%$ and $93 \pm 3\%$ of the DR reactions of the two ions, respectively. The error bars were assessed by varying the integrated area of each peak to extreme values that were still considered to be reasonable and evaluate the matrix system with these values. This was done in conjunction with changing the grid transmission probability within its 3σ confidence interval 0.297 ± 0.015 (Neau 2002).

2.2. Cross sections and rate constant determination

In this part of the experiment the electron velocity in the electron cooler was ramped relative to the ion velocity during the measurement cycle corresponding to a change in collision energy between ~2–1000 meV. The neutral products from the DR reactions were detected with the IID and recorded with a multichannel scaler (MCS), using 2 ms dwell time in such a way that each time interval corresponded to a certain relative collision

energy. Also, neutral particles originating from collisions of the ions with residual gas particles in the ring were collected by a microchannel plate (MCP) detector at the end of a straight section in the ring and recorded by an MCS. Since the intensity of the signals from these background events is directly proportional to the ion current, these signals could be scaled to the absolute ion current which was measured using a capacitive pick up immediately after acceleration (Paal et al. 2006). The ion current could thus be monitored throughout the whole measurement cycle in the ring and therefore could be fitted by a decay curve. This fit could also be used for background subtraction in the cross section measurement. The rate coefficient was then calculated as:

$$k = \left(\frac{\mathrm{d}N}{\mathrm{d}t}\right) \frac{v_i v_e e^2 r_e^2 \pi}{I_e I_i l}, \tag{2}$$

where I_e, v_e and I_i, v_i are the electron and ion currents and velocities (in the laboratory frame), respectively, and $\mathrm{d}N/\mathrm{d}t$ is the measured count rate, e is the elementary charge, r_e is the radius of the electron beam and l is the interaction region length. Due to the high mass difference between the electrons and ions, drag force effects were neglected (Neau 2002). However corrections to the data had to be made for: (a) Space charge effects: The electrons experience a drop in the acceleration potential at the cathode in the cooler due to other electrons ahead of them. (b) Toroidal effects: Ion electron collisions in the regions where the electron beam is bent into and out from the interaction region have higher centre-of-mass energies (E_{cm}) due to the extra transversal velocity components (Lampert et al. 1996). (c) The rate constant including these corrections is an averaged value due to the transversal velocity spread of the electrons (i.e. 2 meV electron temperature). It can therefore be expressed by the equation below through which the actual cross section is deconvoluted using Fourier methods (Mowat et al. 1995):

$$k = \int_0^\infty v_{rel} f(v_\perp) \sigma(v_{rel})\, \mathrm{d}v_\perp, \tag{3}$$

where $f(v_\perp)$ is the transversal electron velocity distribution in the center of mass frame, $v_\perp$ the transversal electron velocity and v_{rel} the relative velocity respectively. The result for the CD_3CDOD^+ ion is displayed in Fig. 3 together with the best fit between 1–200 meV giving a cross section of $\sigma(E_{cm}[\mathrm{eV}]) = 9.2 \pm 4 \times 10^{-16}(E_{cm}[\mathrm{eV}])^{-1.24\pm0.05}$ cm^2. Applying the same procedure for the $CH_3CH_2OH_2^+$ ion (see Fig. 4) resulted in a best fit of: $\sigma(E_{cm}[\mathrm{eV}]) = 1.7 \pm 0.3 \times 10^{-15}(E_{cm}[\mathrm{eV}])^{-1.23\pm0.02}$ cm^2. The thermal reaction rate coefficient can be obtained from the cross sections by applying the formula:

$$k(T) = \frac{8\pi m_e}{(2\pi m_e k_B T)^{3/2}} \int_0^\infty E_{cm}\sigma(E_{cm}) e^{-E_{cm}/k_B T}\, \mathrm{d}E_{cm}, \tag{4}$$

where m_e is the electron mass, k_B, is Boltzmann's constant, T is the electron temperature and E_{cm} is the centre of mass energy. We obtain $k(T) = 1.1 \pm 0.4 \times 10^{-6}(T/300)^{-0.74\pm0.05}$ cm^3 s^{-1} for CD_3CDOD^+ and $k(T) = 1.9 \pm 0.4 \times 10^{-6}(T/300)^{-0.73\pm0.02}$ cm^3 s^{-1} for $CH_3CH_2OH_2^+$. In this evaluation, the errors arise from the uncertainty in the circumference of the ring, the length of the interaction region, the ion and electron currents, the electron density and statistical uncertainty. These combined errors are estimated to be ~33% and ~15% for CD_3CDOD^+ and $CH_3CH_2OH_2^+$, respectively.

We emphasize that the ion temperature is set by the condition at which the cross section was measured in the storage ring. It is reasonable to assume $T_{rot} \approx T_{vib} = 300$ K. Equation (4) can be used to calculate the thermal rate constant for electron temperatures much higher than 300 K but one should note that the equation does not regard excitation of vibrational and rotational states of higher temperatures. However investigations of the dependence of DR rates on vibrational excitation in the case of O_2^+ by Petrignani et al. (2005) showed a change of much less than an order of magnitude.

The influence on the DR process of rotational excitation of the H_3^+ ion was discussed by Tom et al. (2009) where the authors argued that the rate coefficient curve at low electron energy (<10^{-2} eV) could show less structure due to the presence of rotationally hotter ions (dos Santos et al. 2007). Even though less structure was present in the spectra for the hotter ions the overall rate was on the same order. The use of Eq. (4) should therefore be justified. The actual fitting of the cross section was made between 1–200 meV corresponding to a temperature range of 10–2000 K where the spectra are very smooth (although the overall slope is kept up to 1 eV corresponding to over 11 000 K).

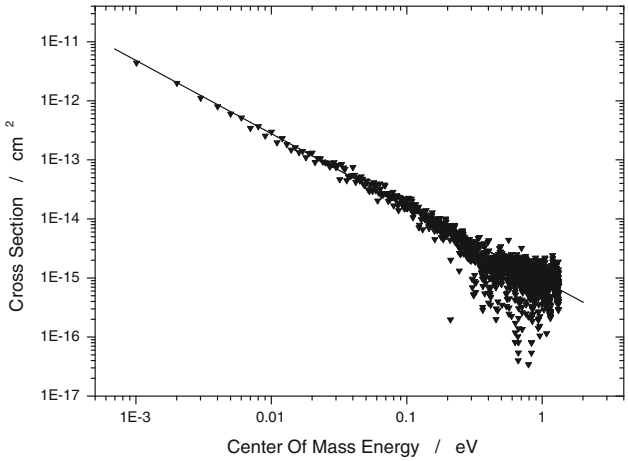

Fig. 3. Cross section of the DR of CD_3CDOD^+ versus relative kinetic energy. The triangles shows individually measured spots while the line shows the best fit between 1–200 meV.

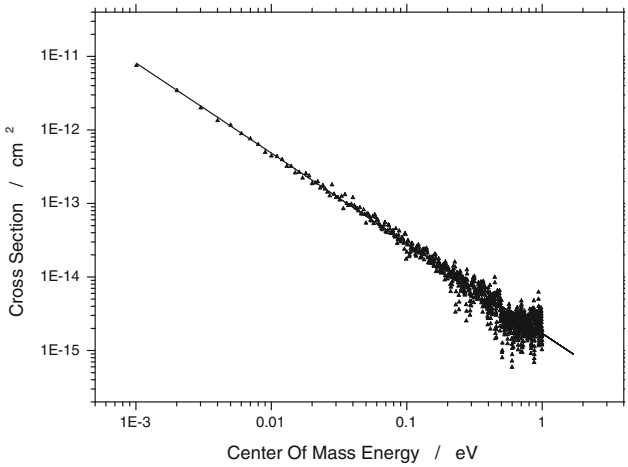

Fig. 4. Cross section of the DR of $CH_3CH_2OH_2^+$ versus relative kinetic energy. The triangles shows individually measured spots while the line shows the best fit between 1–200 meV.

3. Discussion

3.1. The structure of the ions

Both ions were produced from a gas mixture of ethanol and pure hydrogen/deuterium gas in conjunction with a discharge. The ion source is designed and run at a relatively high pressure of ~1 Torr in order to strive for collisional quenching (Österdahl 2006). No vacuum meter is mounted in the ion source, which makes it impossible to measure the relative ethanol/hydrogen pressures. The pressures are instead measured at a position 1.5 m from the source where the base pressure of hydrogen/deuterium in formation of both ions were found to be $\sim 1 \times 10^{-5}$ Torr. The peak pressures after injection of ethanol was found to be $\sim 5 \times 10^{-5}$ Torr. Since the CD_3CDOD^+ ion was generated through fragmentation of fully deuterated ethanol in an atmosphere of D_2 the predominantly occuring formation process should be through electron impact ionization. Four stable main isomers have been reported for the CD_3CDOD^+ ion, of which the titular form is the most stable. The other three (calculated for the hydrogen case) are found within 120 kJ mol^{-1} above the titular isomer (Curtiss et al. 1995): $CH_3OCH_2^+$ (72.4 kJ mol^{-1} above), $CH_2CHOH_2^+$ (95.4 kJ mol^{-1} above), O-protonated ethylene oxide ($CH_2OHCH_2^+$, 116.3 kJ mol^{-1} above) (Curtiss et al. 1995). Formation of the higher-energy $CH_3OCH_2^+$ isomer should be improbable due to the substantial rearrangement implied. However, calculations by Curtiss et al. (1995) show that this isomer can be generated through rearrangement of the unstable singlet $CH_3CH_2O^+$ (50 kJ mol^{-1} above the titular isomer) to $CH_3OCH_2^+$. Interestingly, the isomerisation barrier between this isomer and $CH_2OHCH_2^+$ is calculated to be over the dissociation limit of the ion (Jarrold et al. 1986)). The unstable singlet $CH_3CH_2O^+$ can also relax to a complex between H_2 and H_3CCO^+ while the triplet state of the $CH_3CH_2O^+$ is stable, but energetically lies 393 kJ mol^{-1} above the global minimum and is thus unlikely to be formed in considerable quantities. Other forms such as $CH_3COH_2^+$, CH_3OHCH^+ have been calculated as local minima at 322 and 389 kJ mol^{-1} above the titular isomer (Curtiss et al. 1995). In the current experiment, the ion is created from CH_3CH_2OH (ethanol) and substantial energy and reorganization would be necessary to form an isomer with much higher formation enthalpy from the parent. However, given the complex potential surface of the ions, i.e. having several minima, it is impossible to state with certainty what the population of the given isomers are. Nevertheless, one could assume that the lowest-energy isomer should dominate.

For the $CH_3CH_2OH_2^+$ ion, two formation processes should dominate in the source: 1) Through formation of H_3^+ which occurs readily, followed by protonation of ethanol. 2) Through self-protonation of ethanol in the reaction $CH_3CH_2OH^+ + CH_3CH_2OH \rightarrow CH_3CH_2OH_2^+ + CH_3CH_2O$ which is exothermic with 65 kJ mol^{-1} (Mason & Naylor 1998; Wesdemiotis et al. 1991; Lias et al. 1988). Therefore, the most likely resulting species should be the titular ion ($\Delta_f H$(ion) = 507 kJ mol^{-1}) since formation of the isomeric protonated dimethyl ether ($\Delta_f H$(ion) = 542 kJ mol^{-1}) would not only imply heavy restructuring but also need extra energy (enthalpy values from Lias et al. 1988). Both isomers are stable and the isomerisation barrier is sufficiently high that they can be considered separate species (Matthews & Adams 1997). The schematic potential diagram by Jarrold et al. (1986) clearly shows that the isomerisation barrier is higher than the dissociation energy. This is also the result of a study by Fairley et al. (1997). Complexes such as $C_2H_4.H_3O^+$ calculated to lie 57 kJ mol^{-1} above the titular form cannot be excluded although the isomerisation barrier between the ions is found to be 84 kJ mol^{-1} which is relatively high (Fairley et al. 1997). Following the formation method and the chemistry involved one can assume that the by far dominant ion should be the titular.

3.2. Implications of the branching fractions results for CD_3CDOD^+

Inspection of the branching fraction spectrum for CD_3CDOD^+ (see bottom Fig. 1) allows the conclusion that there are no signals corresponding to mass 6, 12 and 14 amu (3D, C, CD). The exoergic reaction channels are therefore limited to those listed in Table 1 (energies calculated from Lias et al. 1988; and Afeefy et al. 2009), which do not produce fragments with those masses. The only exoergic reaction channels retaining the CCO bonds between the heavy atoms seem to be those that produce a D_2 molecule or one or two deuterium atoms. Together, these processes account for 23% of the reaction flux. The rest of the DR events involve fracture of the CCO-chain into two parts which could be due to a multitude of channels.

Due to the insufficient resolution, it is impossible to obtain an exact distribution of the reaction pathways, although one could obtain a tentative idea by looking at the peak distributions. There seems to be a small amount (zero or close to zero) of products or combinations of lighter fragments with masses of 22, 24, 26 and 34 amu (corresponding to e.g. OD+D_2, D_2O+D_2, C_2D, CD_3O, C_2D_5). Therefore, e.g. the reactions $CD_3CDOD^+ + e^- \rightarrow C_2D_5 + O$ and $CD_3CDOD^+ + e^- \rightarrow C_2D + D_2O + D_2$ do not seem to play a crucial role. On the contrary, the masses 18, 28 and 30 amu seem to be much more important i.e. OD, CO, C_2D_2, DCO, C_2D_3. Reaction channels leading to products with those masses are:

$$CD_3CDOD^+ + e^- \rightarrow CDO + CD_3 + D \quad (5)$$
$$CD_3CDOD^+ + e^- \rightarrow CO + CD_3 + D_2 \quad (6)$$
$$CD_3CDOD^+ + e^- \rightarrow CO + CD_3 + 2D \quad (7)$$
$$CD_3CDOD^+ + e^- \rightarrow C_2D_3 + OD + D \quad (8)$$
$$CD_3CDOD^+ + e^- \rightarrow C_2D_2 + OD + D_2. \quad (9)$$

This does not necessarily mean that all of these pathways are important, but the dominating channels should be amongst them. One should note here that some of the light fragments D and D_2 may acquire sufficient transversal velocity in the DR reaction to bypass the active detector area, which affects the observed distributions of masses in the spectra.

In the previous investigation of DR for the isomeric form $CD_3OCD_2^+$ (Hamberg et al. 2010) we reported that the branching fraction of those channels splitting the COC structure in two heavy fragments was close to unity. The differences are considered to be due to the different structure. This also strengthens our belief that the titular ion isomer dominates in the ion beam.

The measurements were made with the fully deuterated isotopologue of the ion in order to increase the mass resolution to be able to distinguish fragment masses differing with only 2 amu (D). That would make it possible to fit Gaussian functions to each mass peak but due to the insufficient resolution this could not be achieved. In most cases, fully deuterated substances yield similar to identical branching fractions (Jensen et al. 2000; Neau et al. 2000; Geppert et al. 2006), although exceptions exist (Hamberg et al. 2007; Larsson et al. 2005).

3.3. Implications of the branching fractions results for $CH_3CH_2OH_2^+$

From the resulting spectrum for $CH_3CH_2OH_2^+$ with the grid inserted (see Fig. 2) it is clear that we do not see any fragments with mass 12 amu which excludes C from the list of possible products listed in Table 1 (where the energies are calculated from Lias et al. 1988; and Afeefy et al. 2009). Other masses which are not strongly present (zero or close to zero) in the spectrum are 13, 20, 21, 26, 33 and 34 implying low representation of e.g. the following reactions:

$$CH_3CH_2OH_2^+ + e^- \rightarrow C_2H_2 + H_2O + H_2 + H \quad (10)$$
$$CH_3CH_2OH_2^+ + e^- \rightarrow CH_3OH + CH + H_2. \quad (11)$$

Dominating masses are found to be 17–18 amu, 28–30 amu and also 15 amu. This indicates that the especially important DR reactions could be amongst the following:

$$CH_3CH_2OH_2^+ + e^- \rightarrow C_2H_5 + OH + H \quad (12)$$
$$CH_3CH_2OH_2^+ + e^- \rightarrow C_2H_5 + H_2O \quad (13)$$
$$CH_3CH_2OH_2^+ + e^- \rightarrow C_2H_4 + H_2O + H. \quad (14)$$

While the pathways

$$CH_3CH_2OH_2^+ + e^- \rightarrow C_2H_4 + OH + H_2 \quad (15)$$
$$CH_3CH_2OH_2^+ + e^- \rightarrow CH_2O + CH_4 + H \quad (16)$$
$$CH_3CH_2OH_2^+ + e^- \rightarrow CH_2O + CH_3 + H_2 \quad (17)$$
$$CH_3CH_2OH_2^+ + e^- \rightarrow CHO + CH_4 + H_2 \quad (18)$$
$$CH_3CH_2OH_2^+ + e^- \rightarrow CHO + CH_4 + 2H \quad (19)$$
$$CH_3CH_2OH_2^+ + e^- \rightarrow CH_2O + CH_3 + 2H \quad (20)$$
$$CH_3CH_2OH_2^+ + e^- \rightarrow CHO + CH_3 + H_2 + H \quad (21)$$

could also be important, we see much less signals corresponding to masses 16, 19, 31 and 32 amu in our spectrum. This behaviour partly could have its explanation in the fact that some channels could produce H and H_2 fragments with sufficiently high translational kinetic energy to miss the detector, which leads to certain masses being underrepresented in the spectrum.

A comparison with DR investigations of the analogous $CH_3OH_2^+$ ion (Geppert et al. 2006) shows that 19% of DR processes of this ion preserve the CO-structure ($CH_2O + H_2 + H$ 10%, $CH_3O + H_2$ 6%, and $CH_3OH + H$ 3%) compared to 7% retaining the CCO-structure in the case of protonated ethanol. Due to the insufficient resolution it is impossible to exactly resolve the branching fractions between the diffferent reaction pathways for the DR of protonated ethanol. The splitting of the CO-bond occurs in 81% of the DR events of protonated methanol. Here OH and H_2O are the dominant products (appearing in 51% and 30% of the reactions). This also seems to be the case for protonated ethanol.

The previously investigated DR of the isomeric deuteronated dimethyl ether ($CD_3ODCD_3^+$) yielded a splitting of the COC structure into two and three fragments with the probability of 49% and 44% respectively (Hamberg et al. 2010). The large difference in these results is also indicative of the different ion structure in the two experiments.

3.4. Implications of rate constants

The thermal rate constants that are reported here are on the higher end for DR reaction rates which often are around 3×10^{-7} $cm^3\,s^{-1}$ at 300 K for small molecular ions. Nevertheless, there is a clear trend observed from previous investigations that larger ions tend to yield larger rate constants e.g. $C_3H_7^+$ (1.9×10^{-6} $cm^3\,s^{-1}$ Ehlerding et al. 2003) and $DCCCND^+$ (1.5×10^{-6} $cm^3\,s^{-1}$ Geppert et al. 2004).

A direct comparison with the previously investigated isomeric forms show similar rate constants: $k(T) = 1.1 \pm 0.4 \times 10^{-6}\,(T/300)^{-0.74\pm0.05}$ $cm^3\,s^{-1}$ in the case of CD_3CDOD^+compared to $k(T) = 1.7 \pm 0.5 \times 10^{-6}\,(T/300)^{-0.77\pm0.01}$ $cm^3\,s^{-1}$ for $CD_3OCD_2^+$. For $CH_3CH_2OH_2^+$ the rate was $k(T) = 1.9 \pm 0.4\times10^{-6}(T/300)^{-0.73\pm0.02}$ $cm^3\,s^{-1}$ compared to $k(T) = 1.7 \pm 0.6\times10^{-6}$ $(T/300)^{-0.70\pm0.02}$ $cm^3\,s^{-1}$ for $(CD_3)_2OD^+$.

Both ions show a tiny discontinuity in the slope at around 0.3 eV in the cross section spectra (Figs. 3 and 4) which may be due to the opening of different reaction channels including those leading to auto ionisation. The rates at higher relative kinetic energy may, however, also be affected by the background subtraction procedure implying larger errors than in the fitted interval. A

Table 1. Energetically open and plausible reaction channels[a].

CD_3CDOD^+ Products	ΔH (eV)	$CH_3CH_2OH_2^+$ Products	ΔH (eV)
C_2D_4O+D	–5.55	$C_2H_6O + H$	–5.43
$C_2D_3O + D_2$	–6.17	$C_2H_5O + H_2$	–5.94
$C_2D_3O + 2D$	–1.65	$C_2H_5O + 2H$	–1.42
$CD_3O + CD_2$	–2.13	$CH_3CHO + H_2 + H$	–4.76
		$CH_3CHO + 3H$	–0.25
$CD_2O + CD_3$	–5.73		
$CD_2O + CD_2 + D$	–0.98	$CH_3OH + CH_3$	–5.83
		$CH_3OH + CH_2 + H$	–1.07
$CDO + CD_4$	–6.37	$CH_3OH + CH + H_2$	–1.18
$CDO + CD_3 + D$	–1.82		
$CDO + CD_2 + D_2$	–1.59	$CH_3O + CH_4$	–6.12
		$CH_3O + CH_3 + H$	–1.58
$CO + CD_4 + D$	–5.70	$CH_3O + CH_2 + H_2$	–1.34
$CO + CD_3 + D_2$	–5.68		
$CO + CD_3 + 2D$	–1.16	$CH_2O + CH_4 + H$	–4.97
$CO + CD_2 + D_2 + D$	–0.92	$CH_2O + CH_3 + H_2$	–4.95
		$CH_2O + CH_3 + 2H$	–0.43
$C_2D_5 + O$	–2.23	$CH_2O + CH_2 + H_2 + H$	–0.19
$C_2D_4 + OD$	–5.09	$CHO + CH_4 + H_2$	–5.58
$C_2D_4 + O + D$	–0.66	$CHO + CH_4 + 2H$	–1.06
		$CHO + CH_3 + H_2 + H$	–1.03
$C_2D_3 + D_2O$	–5.45		
$C_2D_3 + OD + D$	–0.28	$CO + CH_4 + H_2 + H$	–4.92
$C_2D_3 + O + D_2$	–0.36	$CO + CH_4 + 3H$	–0.40
$C_2D_2 + D_2O + D$	–3.94	$C_2H_5 + H_2O$	–6.53
$C_2D_2 + OD + D_2$	–3.29	$C_2H_5 + OH + H$	–1.36
		$C_2H_5 + O + H_2$	–1.44
$C_2D + D_2O + D_2$	–3.61		
		$C_2H_4 + H_2O + H$	–4.96
		$C_2H_4 + OH + H_2$	–4.31
		$C_2H_3 + H_2O + H_2$	–4.66
		$C_2H_3 + H_2O + 2H$	–0.14
		$C_2H_2 + H_2O + H_2 + H$	–3.15

Notes. [a] Open reaction channels for DR of CD_3CDOD^+ and $CH_3CH_2OH_2^+$. Reaction products and and their respective highest enthalpy of change ΔH is displayed. Enthalpies calculated from values at Lias et al. (1988) and Afeefy et al. (2009).

similar phenomenon has been observed for the previously investigated isomeric forms (Hamberg et al. 2010). Furthermore, in the cross section vs. kinetic energy dependencies of other polyatomic ions a change of slope has also been observed, see e.g. Vigren et al. (2008); Jensen et al. (1999); Zhaunerchyk (2008).

A previous experimental investigation into the DR of CH_3CHOH^+ using the FALP technique showed a rate constant of 3.9×10^{-7} cm^3 s^{-1} at 300 K with a 30% uncertainty (Geoghegan et al. 1991). This is clearly far below our value and we do not currently have an explanation of the large difference between these results. FALP experiments have also been performed to determine the DR rate constant for $CH_3CH_2OH_2^+$ to 1.1×10^{-6} cm^3 s^{-1} at 300 K which is somewhat smaller than our rate constant of 1.9×10^{-6} cm^3 s^{-1} (Adams & Smith 1988).

3.5. Model calculations

The rate constants for both ions are considerably higher than the total rate constants calculated by summing the individual rates of all the DR-reactions used in the Ohio State University and UMIST databases (see Table 2, Garrod et al. 2010; Woodall et al. 2006). More importantly, the branching fractions of the reaction channel leading to preservation of the CCO chain seem to be heavily overestimated in the UDFA model assuming that 50% of the $CH_3CH_2OH_2^+$ ions are forming ethanol, whereas we find that these channels merely amount to 7%. One should also note that the branching fraction of pathways leading to the unprotonated/undeuteronated species only constitute a part of the fraction preserving the CCO structure. In the DR of $CH_3OH_2^+$ the pathway leading to methanol is only 16% of all those DR processes which preserve the CO-bond (Geppert et al. 2006). If one applies the same ratio to the title reaction, only about 1% of the DR reactions would lead to ethanol. This value is not far from the 1.7% assumed in the OSU model. However, the dominating channel (74%) in the OSU model $C_2H_5OH_2^+ + e^- \rightarrow CH_3 + CH_2 + OH + H$ is found to be zero, and should be removed. Also the reaction leading to $CH_3 + CH_2 + H_2O$ should be removed from this model.

For the CH_3CHOH^+ ion we observe 23% CCO fragment conservation whereas the models assume it to be 25% (UDFA) and only 5% (OSU), respectively. Several of the reactions included in the models seem to be inefficient with respect to our results. However, in the OSU model we notice that the product channel leading to CHO + CH_3 + H, with an assumed branching fraction of 45% correlates well with our findings. This processs could probably be complemented by the reaction CO + CH_3 + H_2. Also reactions yielding OD fragments also may play an important role but are not found in either model. It should be worthwhile to undertake new model calculations of star-forming regions including the new branching fractions derived in the present experiments.

Table 2. UDFA and Ohio State Chemical Network rate constants[a] .

Reaction products	α $\times 10^{-7}$	β	Branch. Fract. (%)
OSU			
$CH_3CH_2O^+ + e^- \rightarrow$			
CH_3 + HCO + H	1.35	–0.50	45
CH_2 + H_2CO + H	1.35	–0.50	45
CH_3 + H_2CO	0.150	–0.50	5
CH_3CHO + H	0.150	–0.50	5
Total	3.00	–0.50	100
UDFA			
$CH_3CHOH^+ + e^- \rightarrow$			
CO + CH_4 + H	3.00	–0.50	50
H_2CO + CH_3	1.50	–0.50	25
CH_3CHO + H	1.50	–0.50	25
Total	6.00	–0.50	100
Current data			
$CD_3CDOD^+ + e^- \rightarrow$			
CD_3 + DCO + D	≤8.47	–0.74	≤77
CD_2 + D_2CO + D	≤8.47	–0.74	≤77
CO + CD_4 + D	≤8.47	–0.74	≤77
D_2CO + CD_3	≤8.47	–0.74	≤77
CD_3CDO + D	≤3.00	–0.74	≤23
Total	11	–0.74	100
OSU			
$C_2H_5OH_2^+ + e^- \rightarrow$			
CH_3 + CH_2 + OH + H	6.75	–0.50	74.4
CH_3 + CH_2 + H_2O	0.675	–0.50	7.4
C_2H_5 + OH + H	0.675	–0.50	7.4
C_2H_4 + H_2O + H	0.675	–0.50	7.4
C_2H_5 + H_2O	0.150	–0.50	1.7
C_2H_5OH + H	0.150	–0.50	1.7
Total	9.075	–0.50	100
UDFA			
$CH_3CH_2OH_2^+ + e^- \rightarrow$			
C_2H_4 + H_2O + H	1.50	–0.50	50
C_2H_5OH + H	1.50	–0.50	50
Total	3.00	–0.50	100
Current data			
$CH_3CH_2OH_2^+ + e^- \rightarrow$			
CH_3 + CH_2 + OH + H	0	–0.73	0
CH_3 + CH_2 + H_2O	0	–0.73	0
C_2H_5 + OH + H	≤17.7	–0.73	≤93
C_2H_5 + H_2O	≤17.7	–0.73	≤93
C_2H_4 + H_2O + H	≤17.7	–0.73	≤93
C_2H_5OH + H	≤1.3	–0.73	≤7
Total	19	–0.73	100

Notes. [(a)] Where $k(T) = \alpha^*(T/300)^\beta$ cm^3 s^{-1} and their implied branching fractions. These are compared to the product channel upper limits of the current data.

4. Conclusion

The DR rate coefficients of the investigated ions are relatively high as has been observed with other similarly complex ions. For CD_3CDOD^+ the CCO structure is retained in only 23 ± 3% of the reactions whereas the remainder split into two heavy fragments.

For the DR of $CH_3CH_2OH_2^+$, we report that the dominant fraction (93%) breaks up the CCO chain into two. The branching fraction channel leading to the unprotonated ethanol is found to have an upper limit of 7%. The impact on astrochemical models needs to be assessed.

Acknowledgements. We thank the staff at the Manne Siegbahn Laboratory for making these experiments possible by excellent technical support. W. D. G. thanks the Swedish Research Council for his Senior Researcher grant (contract number 2006-427) and the Swedish Space Board (grant number 76/06). M. K. thanks the Swedish Institute for financial support and also acknowledges support from the Ministry of Science and Higher Education, Poland, under contract N202 111 31/1194. S. T. acknowledges financing from the COST ACTION (CM0805).

References

Adams, N. G., & Smith, D. 1988, Chem. Phys. Lett., 144, 11

Afeefy, H., Liebman, J., & Stein, S. 2009, Neutral Thermochemical Data, NIST Chemistry WebBook, NIST Standard Reference Database Number 69, http://webbook.nist.gov/chemistry

Al-Khalili, A., Danared, H., Larsson, M., et al. 1998, Hyperfine Interact., 114, 281

Andersen, L. H., Heber, O., Kella, D., et al. 1996, Phys. Rev. Lett., 77, 4891, 4894

astrochemistry.net. 2009, http://www.astrochemistry.net

Bisschop, S. E., Fuchs, G. W., van Dishoeck, E. F., & Linnartz, H. 2007, A&A, 474, 1061, 1071

Bisschop, S. E., Jørgensen, J. K., Bourke, T. L., Bottinelli, S., & van Dishoeck, E. F. 2008, A&A, 488, 959

Boger, G. I., & Sternberg, A. 2006, Los Alamos National Laboratory, Preprint Archive, ApJ, 645, 314

Curtiss, L. A., Lucas, D. J., & Pople, J. A. 1995, J. Chem. Phys., 102(8), 3292

Datz, S., Sundström, S., Biedermann, G., et al. 1995, Phys. Rev. Lett., 74, 896, 899

dos Santos, S. F., Kokoouline, V., & Greene, C. H. 2007, J. Chem. Phys., 127, 124309

Ehlerding, A., Arnold, S. T., Viggiano, A. A., et al. 2003, J. Phys. Chem. A, 107, 2179

Fairley, D. A., Scott, G. B. I., Freeman, C. G., Maclagan, R. G. A. R., & McEwan, M. J. 1997, J. Phys. Chem. A, 101, 2848

Florescu-Mitchell, A. I., & Mitchell, J. B. A. 2006, Phys. Rep., 430(5–6), 277

Garrod, R., Weaver, S. L. W., & Herbst, E. 2010, The Ohio State University Astrophysical Chemistry Group, http://www.physics.ohio-state.edu/~eric/research.html

Geoghegan, M., Adams, N. G., & Smith, D. 1991, J. Phys. B: At. Mol. Opt. Phys., 24, 2589

Geppert, W. D., & Larsson, M. 2008, Mol. Phys., 106(16–18), 2199, 2226

Geppert, W. D., Ehlerding, A., Hellberg, F., et al. 2004, ApJ, 613, 1302

Geppert, W. D., Hamberg, M., Thomas, R. D., et al. 2006, Faraday Discuss., 133, 177

Geppert, W. D., Thomas, R. D., Ehlerding, A., et al. 2005, J. Phys. Conf. Ser., 4, 26

Haider, S. A., & Bhardwaj, A. 2005, Icarus, 177(1), 196

Hamberg, M., Geppert, W. D., Rosén, S., et al. 2005, PCCP, 7, 1664

Hamberg, M., Geppert, W. D., Thomas, R. D., et al. 2007, Mol. Phys., 105(5-7), 899

Hamberg, M., Österdahl, F., Thomas, R. D., et al. 2010, A&A, 514, A83

Jarrold, M. F., Kirchner, N. J., Liu, S., & Bowers, M. T. 1986, J. Phys. Chem., 90, 78

Jensen, M. J., Bilodeau, R. C., Heber, O., et al. 1999, Phys. Rev. A: At. Mol. Opt. Phys., 60, 2970

Jensen, M. J., Bilodeau, R. C., Safvan, C. P., Seiersen, K., & Andersen, L. H. 2000, ApJ, 543, 764

Kreckel, H., Motsch, M., Mikosch, J., et al. 2005, Phys. Rev. Lett., 95, 263201

Lampert, A., Wolf, A., Habs, D., et al. 1996, Phys. Rev. A, 53, 1413

Larsson, M., Danared, H., Mowat, J. R., et al. 1993, Phys. Rev. Lett., 70, 430

Larsson, M., Broström, L., Carlson, M., et al. 1995, Phys. Scr., 51, 354

Larsson, M., Ehlerding, A., Geppert, W. D., et al. 2005, J. Chem. Phys., 122, 156101

Lias, S. G., Bartmess, J. E., Liebman, J. F., et al. 1988, J. Phys. Chem. Ref. Data., 17, Suppl. 1

MacDonald, G. H., Gibb, A. G., Habing, R. J., & Millar, T. J. 1996, A&AS, 119, 333

Mason, R. S., & Naylor, J. C. 1998, J. Phys. Chem. A, 102, 10090

Matthews, K. K., & Adams, N. G. 1997, Int. J. Mass. Spectrom. and Ion. Proc., 163, 221

McCall, B. J., Huneycutt, A. J., Saykally, R. J., et al. 2003, Nature, 422, 500

Mitchell, J. B. A., Forand, J. L., Ng, C. T., et al. 1982, Phys. Rev. Lett., 51, 885

Mowat, J. R., Danared, H., Sundström, G., et al. 1995, Phys. Rev. Lett., 74(1), 50

Neau, A. 2002, Ph.D. Thesis, University of Stockholm, Sweden

Neau, A., Al-Khalili, A., Rosén, S., et al. 2000, J. Chem. Phys., 113, 1762

Nevo, I., Novotny, S., Buhr, H., et al. 2007, Phys. rev. A, 76(2, Pt. A), 022713/1

Österdahl, F. 2006, Licentiate thesis, University of Stockholm, Sweden

Paal, A., Simonsson, A., Dietrich, J., & Mohos, I. 2006, Proceedings of EPAC2006, 1196

Peterson, W. K., Abe, T., Fukunishi, H., et al. 1994, J. Geophys. Res., 99(A12), 23257

Petrignani, A., van der Zande, W. J., Cosby, P. C., et al. 2005, Chem. Phys., 122, 014302

Schilke, P., Groesbeck, T. D., Blake, G. A., & Phillips, T. G. 1997, ApJS, 108, 301

Smirnova, N. V., Lyakhov, A. N., & Kozlov, S. I. 2002, Adv. Space Res., 30, 2597

Thomas, R. D. 2008, Mass Spectrom. Rev., 27, 485

Tielens, A. G. G. M., & Charnley, S. B. 1997, Origins Life Evol. B., 27, 23

Tom, B. A., Zhaunerchyk, V., Wiczer, M. B., et al. 2009, J. Chem. Phys., 130, 031101

Vigren, E., Kaminska, M., Hamberg, M., et al. 2008, PCCP, 10, 4014

Wesdemiotis, C., Fura, A., & McLafferty, F. W. 1991, J. Am. Soc. Mass Spectrom, 2, 459

Wolf, A., Krohn, S., Kreckel, H., et al. 2003, Nucl. Instrum. Meth. A, 532, 69

Woodall, J., Agúndez, M., Markwick-Kemper, A. J., & Millar, T. J. 2006, The UMIST Database for Astrochemistry, http://www.udfa.net

Yee, J. H., Abreu, V. J., & Colwell, W. B. 1989, Dissociative Recombination Int. conf., Meeting 1988, 286

Zhaunerchyk, V. 2008, Ph.D. Thesis, University of Stockholm, Sweden